Letter

Medium-assisted enhancement of $\chi_{c1}(3872)$ production from small to large colliding systems

Yu Guo,[1,2] Xingyu Guo,[1,2,*] Jinfeng Liao,[3,†] Enke Wang,[1,2,‡] and Hongxi Xing[1,2,4,§]

[1]*Key Laboratory of Atomic and Subatomic Structure and Quantum Control (MOE), Guangdong Basic Research Center of Excellence for Structure and Fundamental Interactions of Matter, Institute of Quantum Matter, South China Normal University, Guangzhou 510006, China*

[2]*Guangdong-Hong Kong Joint Laboratory of Quantum Matter, Guangdong Provincial Key Laboratory of Nuclear Science, Southern Nuclear Science Computing Center, South China Normal University, Guangzhou 510006, China*

[3]*Physics Department and Center for Exploration of Energy and Matter, Indiana University, 2401 N Milo B. Sampson Lane, Bloomington, Indiana 47408, USA*

[4]*Southern Center for Nuclear-Science Theory (SCNT), Institute of Modern Physics, Chinese Academy of Sciences, Huizhou 516000, China*

(Received 13 February 2023; revised 19 June 2024; accepted 19 July 2024; published 14 August 2024)

Studies of exotic hadrons such as the $\chi_{c1}(3872)$ state provide crucial insights into the fundamental force governing the strong interaction dynamics, with an emerging frontier to investigate their production in high energy collisions where a partonic medium is present. The latest experimental measurements from the Large Hadron Collider show an intriguing evolution pattern of the $\chi_{c1}(3872)$-to-$\psi(2S)$ yield ratio from proton-proton collisions with increasing multiplicities toward proton-lead and lead-lead collisions. Here we propose a mechanism of medium-assisted enhancement for the $\chi_{c1}(3872)$ production, which competes with the more conventional absorption-induced suppression and results in a nonmonotonic trend from small to large colliding systems. Realistic simulations from this model offer a quantitative description of all available data. Predictions are made for the centrality dependence of this observable in PbPb collisions as well as for its system-size dependence from OO and ArAr to XeXe and PbPb collisions. In both cases, a nonmonotonic behavior emerges as the imprint of the competition between enhancement and suppression and can be readily tested by future data.

DOI: 10.1103/PhysRevC.110.L021901

Introduction. The overwhelming majority of the energy and mass in the visible component of our universe comes from the strongly interacting elementary particles, or hadrons, such as protons, neutrons, and pions. According to the fundamental theory of elementary particles known as the Standard Model, these hadrons are themselves made from quarks and antiquarks whose interactions are governed by a basic theory of strong interaction—the quantum chromodynamics (QCD). While the QCD equations are known, their full consequences are difficult to decipher. One of the outstanding challenges is the so-called exotic hadrons, whose quark (antiquark) configurations do not follow the established normal patterns of three quarks forming a baryon (such as the protons and neutrons) and a quark-anti-quark pair forming a meson (like pions).

A most notable example of such states is the $\chi_{c1}(3872)$ particle, also commonly known as $X(3872)$, discovered by the Belle experiment [1] in 2003. Its quark content consists of a pair of charm and anticharm quarks as well as another pair of light flavor quark and antiquark, i.e., $c\bar{c}q\bar{q}$. Subsequently, extensive efforts [2–17] have been made to measure its quantum numbers as well as to find many other candidates of exotic hadrons. There are many open questions in this very active research frontier: What kinds of exotic hadrons could exist? What are the internal structures and properties of them? What are their production and decay mechanism? While properties of $\chi_{c1}(3872)$ have been studied at multiple colliders, physicists remain puzzled by the nature of this particle despite 20 years past its initial discovery, with multiple interpretations being proposed for its internal structures, such as a large-size hadronic molecule versus a compact-size tetraquark state. See recent reviews in, e.g., Refs. [18–28]. Another avenue of investigating exotic hadrons has recently emerged and is rapidly developing, namely, to study their formation in high-energy hadron and nuclear collisions where a partonic medium is present. In such collisions, a fireball with many light flavor quarks (antiquarks) (on the order of hundreds to thousands depending on colliding systems) is created together with a considerable number of charm quarks (antiquarks). This provides an ideal environment for creating heavy flavor exotic states and probing their properties, as demonstrated in the latest theoretical works [29–49]. Most importantly, experimental measurements of $\chi_{c1}(3872)$ production in these collisions have started to arrive in the last few years, including LHCb data from high multiplicity

*Contact author: guoxy@m.scnu.edu.cn
†Contact author: liaoji@indiana.edu
‡Contact author: wangek@scnu.edu.cn
§Contact author: hxing@m.scnu.edu.cn

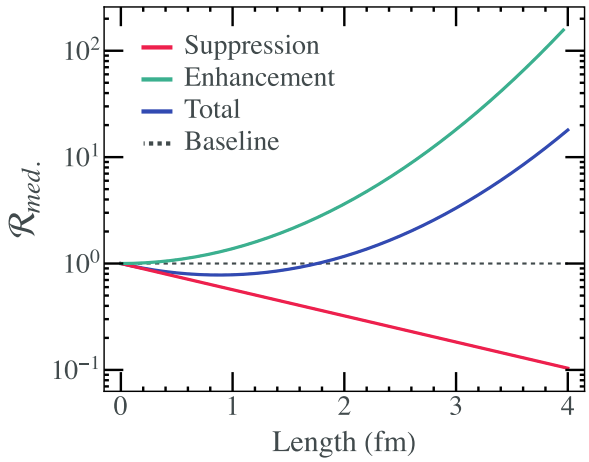

FIG. 1. Individual contributions from absorption-induced suppression (red) and medium-assisted enhancement (green) as well as the overall $\mathcal{R}_{\text{med.}}$ (blue) are plotted as functions of the QGP "brick" length (in fm unit). The QGP is set at a temperature of 360 MeV corresponding to an entropy density of 105 fm^{-3}. The dashed line represents a baseline of $\mathcal{R}_{\text{med.}} = 1$ in the absence of any medium effect.

proton-proton (pp) collisions [50] and proton-lead (pPb) collisions [51], as well as CMS data from lead-lead (PbPb) collisions [8] at the Large Hadron Collider (LHC). Already, this first batch of empirical information shows an unusual pattern of the partonic medium's influence on the $\chi_{c1}(3872)$ yield with respect to the yield of another particle called $\psi(2S)$, which is a normal hadronic state serving as a benchmark for comparison by virtue of its similar heavy flavor content and decay channel ($J/\Psi\pi\pi$) as well as close mass value to the exotic $\chi_{c1}(3872)$. (These data points are shown in Fig. 2.) The LHCb pp results suggest the yield ratio of $\chi_{c1}(3872)$ relative to $\psi(2S)$ decreases with increasing event multiplicity, which

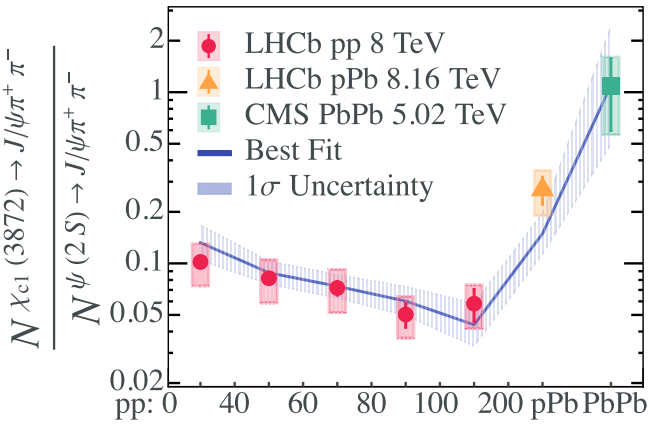

FIG. 2. A comparison of the $\chi_{c1}(3872)$ yield relative to $\psi(2S)$ between model simulation results (blue curve) and experimental data from LHCb pp collisions at $\sqrt{S_{NN}} = 8$ TeV (red circle), LHCb pPb collisions at $\sqrt{S_{NN}} = 8.16$ TeV (orange triangle), and CMS PbPb collisions at $\sqrt{S_{NN}} = 5.02$ TeV (green box) [8,50,51]. The model parameters are determined from the global fitting analysis with the blue band showing the 1σ level uncertainty. (See text for details.)

would hint at a suppression effect due to the medium. On the other hand, the LHCb pPb results and the CMS PbPb results, for which the generated medium is expected to be larger in terms of parton density and system size as compared with pp collisions, show a strong increase in this observable, which would indicate an opposite trend to the pp results. So far, there has lacked a consistent explanation that reconciles this intriguing behavior of $\chi_{c1}(3872)$ production from small to large colliding systems. In this Letter, we present a phenomenological model for the partonic medium attenuation effects on the production of $\chi_{c1}(3872)$ in high energy hadron and nuclear collisions. In particular, a mechanism of medium-assisted enhancement effect will be proposed which competes with the more conventional absorption-induced suppression effect. Based on this important feature, it will first be demonstrated qualitatively how the competition leads to a nontrival pattern in the yield ratio of $\chi_{c1}(3872)$ relative to the $\psi(2S)$ while the partonic medium evolves from the smaller to the larger systems. We will then utilize realistic simulations to show how such a model offers the first quantitative description of all available experimental data. Predictions will also be made for observables that can be verified in the future.

Method. In the high p_T region where recent CMS and LHCb measurements were made, the production of $\psi(2S)$ and $\chi_{c1}(3872)$ should dominantly come from virtual $c\bar{c}$ pairs generated in the initial hard scatterings. Suppose the number of such pairs that would eventually turn into $\psi(2S)$ and $\chi_{c1}(3872)$, in the absence of any medium effect, would be $N_{\psi(2S)}$ and N_X, respectively. However, in nucleus-nucleus (AA) or high-multiplicity pp and proton-nucleus (pA) collisions, these pairs will need to first travel through the created partonic medium before producing those final hadrons. The influence of the medium on the evolution of such $c\bar{c}$ pairs is the focus of our analysis.

The first important effect is the medium absorption. Random collisions with quarks and gluons from the medium result in the dissociation of the correlated comoving $c\bar{c}$ pair, which is akin to the well-known J/Ψ suppression as well as jet quenching that have been observed in AA collisions [52,53].

We model this effect as the geometric absorption along the in-medium path of a $c\bar{c}$ pair,

$$\frac{\mathrm{d}N_i}{\mathrm{d}x} = -\alpha_i n(x) N_i, \tag{1}$$

where $i \to \psi(2S), \chi_{c1}(3872)$. The $n(x)$ is the local parton density of the medium along the path of a surviving $c\bar{c}$ pair. The coefficient α_i describes the likelihood of a given state to be dissociated, with the dimension of a cross section. In the studies of production for normal charmonium and bottomonium states, it is often assumed that higher mass states with less binding energy would suffer stronger absorption effect [52–57]. However, given the theoretical uncertainty concerning $\chi_{c1}(3872)$ structures, let us *not* assume the relative relation of absorption effect between $\chi_{c1}(3872)$ and $\psi(2S)$ and use experimental data to determine this. As is typically done in geometric models for jet energy loss or for charmonium suppression, one can evaluate the overall suppression by first integrating the above equation along any given path, then averaging over all possible in-medium paths, and finally

averaging over collision events. This leads to the following expression for the suppression factor of $\psi(2S)$:

$$R^{\psi(2S)} = \langle\langle e^{-\alpha_{\psi(2S)}\int_{\rm path} n(x){\rm d}x}\rangle\rangle, \tag{2}$$

where the notation $\langle\langle ...\rangle\rangle$ means $\langle\langle ...\rangle_{\rm path}\rangle_{\rm event}$. We note that such a suppression effect applies similarly to the $\chi_{c1}(3872)$ production. For $\chi_{c1}(3872)$, however, there is another medium effect that can actually help enhance its production. In addition to the $c\bar{c}$, the formation of $\chi_{c1}(3872)$ requires two light quarks (antiquarks). Scatterings with the partonic medium, which serves as a reservoir of numerous light quarks (antiquarks), could lead to "picking up" of light quarks (antiquarks) which then comove with the $c\bar{c}$ pair. This enhances the probability to form the $\chi_{c1}(3872)$ state in the end. One could consider this as a two-step process, in which the $c\bar{c}$ pair picks up the first needed light parton and subsequently a second needed light parton. Therefore, one can model such a *medium-assisted enhancement* effect as follows:

$$\frac{{\rm d}N_{\chi_{c1}}}{{\rm d}x} = \beta_X n(x)\left[\int_0^x \beta_X n(y){\rm d}y\right]N_X, \tag{3}$$

where β_X is a parameter characterizing the probability of picking up a single light parton, which also has the dimension of a cross section. An important feature of this effect is that it scales as square power of the medium parton density. We note the enhancement mechanism here differs from the so-called regeneration or recombination mechanism [52,57–61] in several aspects. The former utilizes light partons from thermal plasma to help the formation of exotic states while the latter generates normal charmonia states with individual c and c-bar quarks that are produced in initial hard scatterings and evolve along with bulk medium. The regeneration occurs at the instance of hadronization while the enhancement mechanism here happens through the continuous interactions between the $c\bar{c}$ pairs with thermal partons along their whole paths traversing the medium. The proposed mechanism bears similarity with the recombination effect in the comovers-interaction model (see, e.g., Ref. [59]) in the sense that they both can bring difference to the production of $\chi_{c1}(3872)$ and $\psi(2S)$. However, the recombination effect is more significant in the low p_T region, while our mechanism is dominant in the high p_T region.

Combining this enhancement together with the previous suppression effect, one obtains

$$R^X = \langle\langle e^{\int_{\rm path}[-\alpha_X n(x)+\beta_X^2 n(x)\int_0^x n(y){\rm d}y]{\rm d}x}\rangle\rangle. \tag{4}$$

The two parameters α_X and β_X quantify the suppression and enhancement due to dynamical interactions with medium. Their values should be sensitive to whether the $\chi_{c1}(3872)$ is a hadronic molecule or a tetraquark state. Thus, extracting them from experimental data can help shed light on the microscopic structure of $\chi_{c1}(3872)$.

Now we can compare the production of $\chi_{c1}(3872)$ relative to $\psi(2S)$. This is quantified by the ratio of their baseline pp production cross section, modulated by their respective suppression (enhancement) effects along the in-medium paths:

$$\frac{N^X}{N^{\psi(2S)}} = \frac{\sigma_{pp}^X}{\sigma_{pp}^{\psi(2S)}}\times\frac{R^X}{R^{\psi(2S)}} \approx \frac{\sigma_{pp}^X}{\sigma_{pp}^{\psi(2S)}}\times\mathcal{R}_{\rm med.}, \tag{5}$$

$$\mathcal{R}_{\rm med.} \equiv \langle\langle e^{\int_{\rm path}[-(\alpha_X-\alpha_{\psi(2S)})n(x)+\beta_X^2 n(x)\int_0^x n(y){\rm d}y]{\rm d}x}\rangle\rangle. \tag{6}$$

In the above, the pp baseline $\sigma_{pp}^X/\sigma_{pp}^{\psi(2S)}$ could be inferred from experimental data. We will focus on analyzing the medium attenuation factor $\mathcal{R}_{\rm med.}$. Clearly, $\mathcal{R}_{\rm med.} > 1$ implies an overall medium enhancement while $\mathcal{R}_{\rm med.} < 1$ means an overall medium suppression for the $\chi_{c1}(3872)$ production relative to the $\psi(2S)$. While the individual yield of $\chi_{c1}(3872)$ and $\psi(2S)$ separately could provide useful information, we focus on their yield ratio in the present study, which is the observable measured by LHCb and CMS and which could help reveal unique features of exotic hadron production by comparison with $\psi(2S)$.

Let us first examine the qualitative feature of the partonic medium effect under the assumption of $\alpha_X > \alpha_{\psi(2S)}$ and thus $\alpha_X - \alpha_{\psi(2S)} > 0$, in which case the first term in the exponential of $\mathcal{R}_{\rm med.}$ is a suppression term (— note though in the later fitting analysis we do *not* assume this). Its contribution grows linearly with the medium parton density and the path length. The second term is an enhancement term and its contribution grows quadratically with the parton density and path length. As a result, for relatively low medium density and/or small medium size, the first term will dominate and therefore the overall medium effect would be a suppression of $\chi_{c1}(3872)$ relative to $\psi(2S)$. On the other hand, for relatively high medium density and large medium size, the second term will dominate and therefore the overall medium effect would be an enhancement, instead. This nonlinear feature, arising from the competition between suppression and enhancement, points to a nonmonotonic evolution of medium effect that can help explain and provide a unified interpretation of the recent measurements by both LHCb and CMS from small to large colliding systems. For a simple illustration, let us assume that the average medium effect can be approximated by an average parton density $\bar{n}$ and average path length $\bar{L}$. Further defining a medium thickness parameter $\bar{W} \equiv \bar{n}\cdot\bar{L}$, the factor $\mathcal{R}_{\rm med.}$ can be simplified as

$$\mathcal{R}_{\rm med.} = e^{[-(\alpha_X-\alpha_{\psi(2S)})\bar{W}+\frac{1}{2}\beta_X^2\bar{W}^2]}. \tag{7}$$

The above result clearly suggests that changing from pp with increasing multiplicities through pA eventually to AA collisions, the medium thickness $\bar{W}$ will monotonically increase so that the medium attenuation factor $\mathcal{R}_{\rm med.}$ should first decrease and then increase, for which a minimum would occur at $\bar{W} = \bar{n}\bar{L} = \frac{\alpha_X-\alpha_{\psi(2S)}}{\beta_X^2}$. To further demonstrate this feature, let us compute the $\mathcal{R}_{\rm med.}$ for such a simple partonic medium, essentially a QGP brick [62] with constant and homogeneous temperature which extends along a given direction with a fixed width. In Fig. 1, the individual contributions from suppression term (red) and enhancement term (green) as well as the overall $\mathcal{R}_{\rm med.}$ (blue) are plotted as functions of the QGP brick length, showing the nontrivial decrease-then-increase behavior of $\mathcal{R}_{\rm med.}$ due to the competition between suppression

and enhancement. This behavior already qualitatively agrees with the trends seen in experimental data.

Of course, the partonic medium created in those collisions is much more complicated than the simple approximation here, due to nontrivial initial conditions, event-by-event fluctuations, dynamical expansions, etc. To fully verify the feasibility of this idea, one needs to perform quantitative and realistic simulations, which we report next.

One important issue not discussed so far is the kinematic factors such as transverse momentum. The geometric path approach here is suitable for describing a rapidly traversing probe. The exact value of the probe's momentum does not affect its path too much, therefore the momentum dependence of the enhancement (suppression) effects here is ignored as a first approximation.

Results. To quantitatively evaluate the medium effect on the $\chi_{c1}(3872)$ production relative to the $\psi(2S)$, we utilize event-by-event simulations based on the iEBE-VISHNU hydrodynamic model [63], which has been well tested by experimental data from small to large colliding systems [64–107]. The iEBE-VISHNU provides eventwise time-dependent evolution information of the bulk medium as well as initial conditions for pp, pA, and AA collisions. We generate $c\bar{c}$ pairs at different spots on the event plane according to the initial binary collision density profiles. The pairs then move along straight paths whose directions are randomly chosen, and along each path the bulk medium is evolving in time. At each spacetime point, the local entropy density can be read from the iEBE-VISHNU hydrodynamic evolution, which is directly related to active degrees of freedom in the thermal medium and thus can be used to represent the local parton density up to a proportionality constant. In this paper, we simulated a total of 500 000 events for pp collisions at $\sqrt{S_{NN}} = 8$ TeV, 200 000 events for pPb collisions at $\sqrt{S_{NN}} = 8.16$ TeV, and 100 000 events for PbPb collisions at $\sqrt{S_{NN}} = 5.02$ TeV. Model parameters of the hydro code were set in the same way as previous studies based on the same package in the literature, see, e.g., Refs. [66,83,89]. The bulk properties such as multiplicity and elliptic flow from our simulations compare well with experimental measurements for all colliding systems. For each event, we further simulate about 100 to 10 000 in-medium paths depending on the medium size. Due to the substantial amount of needed computing time, we chose to simplify the calculations by first performing average over the path integrations in each event and then computing the exponential for the ratio between $\chi_{c1}(3872)$ and $\psi(2S)$. That is,

$$\mathcal{R}_{\text{med.}} \approx \langle e^{-\alpha' \cdot P_1 + \beta'^2 \cdot P_2} \rangle_{\text{event}}, \tag{8}$$

where

$$P_1 = \left\langle \int_{\text{path}} s(x) \mathrm{d}x \right\rangle_{\text{path}}, \tag{9}$$

$$P_2 = \left\langle \int_{\text{path}} s(x) \left(\int_0^x s(y) \mathrm{d}y \right) \mathrm{d}x \right\rangle_{\text{path}}, \tag{10}$$

where we introduce $s(x)$ as the entropy density, and $\alpha' = (\alpha_X - \alpha_{\psi(2S)})(\frac{n}{s})$, $\beta' = \beta_X(\frac{n}{s})$, whose definitions absorb the proportionality constant between parton density and entropy density.

To determine the two key parameters α' and β', we take the LHCb pp (at $\sqrt{S_{NN}} = 8$ TeV) and preliminary pPb (at $\sqrt{S_{NN}} = 8.16$ TeV) as well as the CMS PbPb (at $\sqrt{S_{NN}} = 5.02$ TeV) data for a global fitting analysis, with results shown in Fig. 2. The best fit, with $\chi^2/d.o.f = 1.78$, gives the following numbers with 1σ level uncertainty: $\alpha' = (5.7 \pm 2.2) \times 10^{-3}$ fm^2, $\beta' = (5.7 \pm 0.7) \times 10^{-3}$ fm^2, and $\sigma^X_{pp}/\sigma^{\psi(2S)}_{pp} = 0.162 \pm 0.037$. Note that the data from LHCb and CMS have different p_T regions (with $p_T > 5$ GeV for the former and 15 GeV $< p_T <$ 50 GeV for the latter), but as mentioned above, this would not affect our current model simulation. As one can see, our model with just two parameters characterizing a competition between suppression and enhancement can well describe the quantitative trends of all global data from small to large systems. The proposed medium-assisted enhancement is particularly important for understanding the rapid increase of $\chi_{c1}(3872)$ yield relative to $\psi(2S)$ in the pPb and PbPb collisions. It would be interesting to compare the obtained medium effect in this model with that from the comover-interaction model in Ref. [35]. In our model, the medium effect is controlled by the α', β' coefficients multiplied by local entropy density and in-medium path length, with an average estimate $\approx$0.6. In the model of Ref. [35], the control quantity is the product of velocity, cross section, and transverse comover density, with an average estimate $\approx$0.7. The two demonstrate qualitative consistency. The phenomenological extraction of the two parameters from experimental data can serve as important constraints on the nature of $\chi_{c1}(3872)$. Microscopic calculations of these parameters based on different assumptions (e.g., hadronic molecule versus tetraquark state) could then be compared with the empirical values obtained here to help decipher its internal structures.

A natural next step would be testing our model predictions for which experimental data are not yet available and can serve as a future validation. To do that, we further investigate the centrality dependence of the medium effect in the PbPb collisions. In Fig. 3, we show the yield ratio of $\chi_{c1}(3872)$ to $\psi(2S)$ in three centrality bins: $60-90\%$, $30-60\%$, and $0-30\%$. Interestingly, the results again show a nonmonotonic behavior. In peripheral collisions, the ratio is about 0.1, while in the middle-centrality class it will drop to around 0.02, which is comparable to that in the pPb collisions. Finally, in the central collisions, it rockets up to be as high as 3. This finding also suggests that the most central collisions actually contribute most of the $\chi_{c1}(3872)$ particles observed in the minimal bias measurements from CMS. We emphasize that the model parameters were already fixed in the aforementioned fitting analysis, so the highly nontrivial centrality trend predicted by the model here will be an important verification by future measurements.

Finally, the system size scan for AA collisions could offer yet another independent validation of our model predictions. For that purpose, we have computed the $\chi_{c1}(3872)$ to $\psi(2S)$ yield ratio for the following systems: OO collisions at $\sqrt{S_{NN}} = 6.5$ TeV, ArAr collisions at $\sqrt{S_{NN}} = 5.85$ TeV, and XeXe collisions at $\sqrt{S_{NN}} = 5.44$ TeV. These results

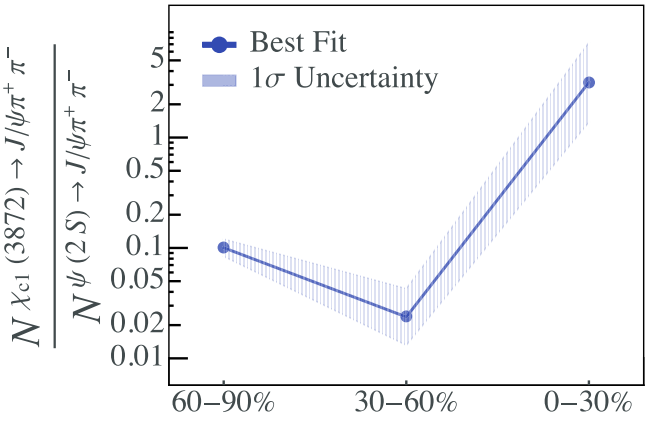

FIG. 3. The predicted centrality dependence of the $\chi_{c1}(3872)$ yield relative to $\psi(2S)$ in PbPb collisions at $\sqrt{S_{NN}} = 5.02$ TeV collisions. The blue uncertainty band is from the same source as in Fig. 2.

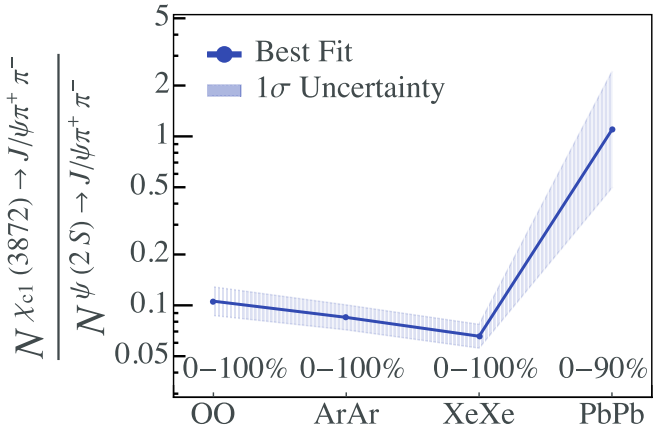

FIG. 4. The predicted trend of the $\chi_{c1}(3872)$ yield relative to $\psi(2S)$ in AA collisions from small to large systems, including OO collisions at $\sqrt{S_{NN}} = 6.5$ TeV, ArAr collisions at $\sqrt{S_{NN}} = 5.85$ TeV, XeXe collisions at $\sqrt{S_{NN}} = 5.44$ TeV, as well as PbPb collisions at $\sqrt{S_{NN}} = 5.02$ TeV. The blue uncertainty band is from the same source as in Fig. 2.

are shown in Fig. 4 in comparison with PbPb collisions at $\sqrt{S_{NN}} = 5.02$ TeV. Again, one observes a nontrivial trend that first decreases and then increases when changing from smaller to larger colliding systems. Such prediction of the system size dependence in AA collisions can be readily tested with future measurements.

Conclusion. To conclude, we present a phenomenological model for the partonic medium attenuation effects on the production of $\chi_{c1}(3872)$ and $\psi(2S)$ particles in high energy hadron and nuclear collisions. In particular, a unique mechanism of medium-assisted enhancement effect is proposed for the $\chi_{c1}(3872)$ production, which leads to a competition with the more conventional absorption-induced suppression effect and becomes more dominant for higher parton densities and larger medium size. As a consequence of this important feature, the yield ratio of $\chi_{c1}(3872)$ relative to the $\psi(2S)$ develops a nontrivial pattern, first decreasing then increasing, when the partonic medium evolves from small to large colliding systems. Utilizing realistic simulations, we show that this model offers a quantitative description of all available experimental measurements, including the LHCb pp (at $\sqrt{S_{NN}} =$ 8 TeV) and preliminary pPb (at $\sqrt{S_{NN}} = 8.16$ TeV) as well as the CMS PbPb (at $\sqrt{S_{NN}} = 5.02$ TeV) data. We further make predictions for the centrality dependence of the $\chi_{c1}(3872)$-to-$\psi(2S)$ yield ratio in PbPb collisions as well as for its system size dependence from OO and ArAr to XeXe and PbPb collisions. In both cases, a nonmonotonic pattern emerges as the imprint of the competition between enhancement and suppression. Given the expected abundance of experimental data from planned runs as well as anticipated upgrades at the LHC, it would be exciting to test these predictions with future high-precision measurements. Last but not least, while the present paper focuses on $\chi_{c1}(3872)$ production, the medium-assisted enhancement mechanism could be applicable to the production of other similar exotic hadrons.

Acknowledgments. This research was supported in part by the National Natural Science Foundation of China (NSFC) under Grants No. 12035007, No. 12022512, and No. 11905066, by Guangdong Major Project of Basic and Applied Basic Research No. 2020B0301030008, by the National Science Foundation in U.S. under Grant No. PHY-2209183 (J.L.), and by the DOE through ExoHad Topical Collaboration.

[1] S. K. Choi *et al.* (Belle Collaboration), Observation of a narrow charmonium-like state in exclusive $B^{\pm} \to K^{\pm}\pi^{+}\pi^{-}J/\psi$ decays, Phys. Rev. Lett. **91**, 262001 (2003).

[2] D. Acosta *et al.* (CDF II Collaboration), Observation of the narrow state $X(3872) \to J/\psi\pi^{+}\pi^{-}$ in $\bar{p}p$ collisions at $\sqrt{s} =$ 1.96 TeV, Phys. Rev. Lett. **93**, 072001 (2004).

[3] V. M. Abazov *et al.* (D0 Collaboration), Observation and properties of the $X(3872)$ decaying to $J/\psi\pi^{+}\pi^{-}$ in $p\bar{p}$ collisions at $\sqrt{s} = 1.96$ TeV, Phys. Rev. Lett. **93**, 162002 (2004).

[4] R. Aaij *et al.* (LHCb Collaboration), Study of the lineshape of the $\chi_{c1}(3872)$ state, Phys. Rev. D **102**, 092005 (2020).

[5] R. Aaij *et al.* (LHCb Collaboration), Study of the $\psi_2(3823)$ and $\chi_{c1}(3872)$ states in $B^{+} \to (J\psi\pi^{+}\pi^{-})K^{+}$ decays, J. High Energy Phys. 08 (2020) 123.

[6] M. Ablikim *et al.* (BESIII Collaboration), Study of open-charm decays and radiative transitions of the $X(3872)$, Phys. Rev. Lett. **124**, 242001 (2020).

[7] M. Ablikim *et al.* (BESIII Collaboration), Observation of $e^{+}e^{-} \to \gamma X(3872)$ at BESIII, Phys. Rev. Lett. **112**, 092001 (2014).

[8] A. M. Sirunyan *et al.* (CMS Collaboration), Evidence for X(3872) in Pb-Pb collisions and studies of its prompt production at $\sqrt{s_{NN}}$=5.02 TeV, Phys. Rev. Lett. **128**, 032001 (2022).

[9] J. P. Lees *et al.* (BaBar Collaboration), Measurements of the absolute branching fractions of $B^{\pm} \to K^{\pm} X_{c\bar{c}}$, Phys. Rev. Lett. **124**, 152001 (2020).

[10] Y. Kato *et al.* (The Belle Collaboration), Measurements of the absolute branching fractions of $B^+ \to X_{c\bar{c}} K^+$ and $B^+ \to \bar{D}^{(*)0}\pi^+$ at Belle, Phys. Rev. D **97**, 012005 (2018).

[11] C. Li and C.-Z. Yuan, Determination of the absolute branching fractions of X(3872) decays, Phys. Rev. D **100**, 094003 (2019).

[12] M. Ablikim *et al.* (BESIII Collaboration), Search for$X(3872) \to \pi^0 \chi_{c0}$ and $X(3872) \to \pi\pi\chi_{c0}$ at BESIII, Phys. Rev. D **105**, 072009 (2022).

[13] J. H. Yin *et al.* (Belle Collaboration), Search for $X(3872) \to \pi^+\pi^-\pi^0$ at Belle, Phys. Rev. D **107**, 052004 (2023).

[14] R. Aaij *et al.* (LHCb Collaboration), Observation of sizeable ω contribution to $\chi_{c1}(3872) \to \pi^+\pi^- J/\psi$ decays, Phys. Rev. D **108**, L011103 (2023).

[15] B. Aubert *et al.* (The BaBar Collaboration), Evidence for $X(3872) \to \psi_{2S}\gamma$ in $B^{\pm} \to X_{3872} K^{\pm}$ decays, and a study of $B \to c\bar{c}\gamma K$, Phys. Rev. Lett. **102**, 132001 (2009).

[16] V. Bhardwaj *et al.* (Belle Collaboration), Observation of $X(3872) \to J/\psi\gamma$ and search for $X(3872) \to \psi'\gamma$ in B decays, Phys. Rev. Lett. **107**, 091803 (2011).

[17] R. Aaij *et al.* (LHCb Collaboration), Evidence for the decay $X(3872) \to \psi(2S)\gamma$, Nucl. Phys. B **886**, 665 (2014).

[18] N. Brambilla, S. Eidelman, B. K. Heltsley, R. Vogt, G. T. Bodwin, E. Eichten, A. D. Frawley, A. B. Meyer, R. E. Mitchell, V. Papadimitriou *et al.*, Heavy quarkonium: progress, puzzles, and opportunities, Eur. Phys. J. C **71**, 1534 (2011).

[19] A. Esposito, A. L. Guerrieri, F. Piccinini, A. Pilloni, and A. D. Polosa, Four-quark hadrons: an updated review, Int. J. Mod. Phys. A **30**, 1530002 (2015).

[20] R. A. Briceño, T. D. Cohen, S. Coito, J. J. Dudek, E. Eichten, C. S. Fischer, M. Fritsch, W. Gradl, A. Jackura, M. Kornicer *et al.*, Issues and opportunities in exotic hadrons, Chin. Phys. C **40**, 042001 (2016).

[21] M. R. Shepherd, J. J. Dudek, and R. E. Mitchell, Searching for the rules that govern hadron construction, Nature (London) **534**, 487 (2016).

[22] A. Hosaka, T. Iijima, K. Miyabayashi, Y. Sakai, and S. Yasui, Exotic hadrons with heavy flavors: X, Y, Z, and related states, Prog. Theor. Exp. Phys **2016**, 062C01 (2016).

[23] A. Esposito, A. Pilloni, and A. D. Polosa, Multiquark resonances, Phys. Rep. **668**, 1 (2017).

[24] R. F. Lebed, R. E. Mitchell, and E. S. Swanson, Heavy-quark QCD exotica, Prog. Part. Nucl. Phys. **93**, 143 (2017).

[25] S. L. Olsen, T. Skwarnicki, and D. Zieminska, Nonstandard heavy mesons and baryons: Experimental evidence, Rev. Mod. Phys. **90**, 015003 (2018).

[26] F.-K. Guo, C. Hanhart, U.-G. Meißner, Q. Wang, Q. Zhao, and B.-S. Zou, Hadronic molecules, Rev. Mod. Phys. **90**, 015004 (2018) [Rev. Mod. Phys. **94**, 029901(E) (2022)].

[27] T.-W. Wu, Y.-W. Pan, M.-Z. Liu, and L.-S. Geng, Multi-hadron molecules: Status and prospect, Sci. Bull. **67**, 1735 (2022).

[28] H.-X. Chen, W. Chen, X. Liu, Y.-R. Liu, and S.-L. Zhu, An updated review of the new hadron states, Rep. Prog. Phys. **86**, 026201 (2023).

[29] S. Cho *et al.* (ExHIC Collaboration), Multi-quark hadrons from heavy ion collisions, Phys. Rev. Lett. **106**, 212001 (2011).

[30] S. Cho *et al.* (ExHIC Collaboration), Studying exotic hadrons in heavy ion collisions, Phys. Rev. C **84**, 064910 (2011).

[31] S. Cho *et al.* (ExHIC Collaboration), Exotic hadrons from heavy ion collisions, Prog. Part. Nucl. Phys. **95**, 279 (2017).

[32] J. Hong, S. Cho, T. Song, and S. H. Lee, Hadronic effects on the $cc\bar{q}\bar{q}$ tetraquark state in relativistic heavy ion collisions, Phys. Rev. C **98**, 014913 (2018).

[33] C. E. Fontoura, G. Krein, A. Valcarce, and J. Vijande, Production of exotic tetraquarks $QQ\bar{q}\bar{q}$ in heavy-ion collisions at the LHC, Phys. Rev. D **99**, 094037 (2019).

[34] H. Zhang, J. Liao, E. Wang, Q. Wang, and H. Xing, Deciphering the nature of X(3872) in heavy ion collisions, Phys. Rev. Lett. **126**, 012301 (2021).

[35] A. Esposito, E. G. Ferreiro, A. Pilloni, A. D. Polosa, and C. A. Salgado, The nature of $X(3872)$ from high-multiplicity pp collisions, Eur. Phys. J. C **81**, 669 (2021).

[36] E. Braaten, L.-P. He, K. Ingles, and J. Jiang, Production of $X(3872)$ at high multiplicity, Phys. Rev. D **103**, L071901 (2021).

[37] B. Wu, X. Du, M. Sibila, and R. Rapp, $X(3872)$ transport in heavy-ion collisions, Eur. Phys. J. A **57**, 314(E) (2021).

[38] L. M. Abreu and F. J. Llanes-Estrada, Heating triangle singularities in heavy ion collisions, Eur. Phys. J. C **81**, 430 (2021).

[39] Y. Hu, J. Liao, E. Wang, Q. Wang, H. Xing, and H. Zhang, Production of doubly charmed exotic hadrons in heavy ion collisions, Phys. Rev. D **104**, L111502 (2021).

[40] B. Chen, L. Jiang, X.-H. Liu, Y. Liu, and J. Zhao, $X(3872)$ production in relativistic heavy-ion collisions, Phys. Rev. C **105**, 054901 (2022).

[41] M. Albaladejo, J. M. Nieves, and L. Tolos, $D\bar{D}^*$ scattering and $\chi_{c1}(3872)$ in nuclear matter, Phys. Rev. C **104**, 035203 (2021).

[42] H.-g. Xu, Z.-L. She, D.-M. Zhou, L. Zheng, X.-L. Kang, G. Chen, and B.-H. Sa, Investigation of exotic state $X(3872)$ in pp collisions at $\sqrt{s} = 7$, 13 TeV, Eur. Phys. J. C **81**, 784 (2021).

[43] L. M. Abreu, F. S. Navarra, M. Nielsen, and H. P. L. Vieira, Interactions of the doubly charmed state T_{cc}^+ with a hadronic medium, Eur. Phys. J. C **82**, 296 (2022).

[44] Y. Jin, S.-Y. Li, Y.-R. Liu, Q. Qin, Z.-G. Si, and F.-S. Yu, Color and baryon number fluctuation of preconfinement system in production process and T_{cc} structure, Phys. Rev. D **104**, 114009 (2021).

[45] L. M. Abreu, H. P. L. Vieira, and F. S. Navarra, Multiplicity of the doubly charmed state T_{cc}^+ in heavy-ion collisions, Phys. Rev. D **105**, 116029 (2022).

[46] E. Braaten, R. Bruschini, L.-P. He, K. Ingles, and J. Jiang, Evolution of charm-meson ratios in an expanding hadron gas, Phys. Rev. D **107**, 076006 (2023).

[47] H. Yun, D. Park, S. Noh, A. Park, W. Park, S. Cho, J. Hong, Y. Kim, S. Lim, and S. H. Lee, $X(3872)$ and T_{cc}: Structures and productions in heavy ion collisions, Phys. Rev. C **107**, 014906 (2023).

[48] G. Montaña, A. Ramos, L. Tolos, and J. M. Torres-Rincon, The $X(3872)$, the $X(4014)$, and their bottom partners at finite temperature, Phys. Rev. D **107**, 054014 (2023).

[49] Y. Hu and H. Zhang, The production of $X_{cs\bar{c}\bar{s}}$ in heavy ion collisions, Chin. Phys. C, **47**, 051001 (2023).

[50] R. Aaij *et al.* (LHCb Collaboration), Observation of multiplicity dependent prompt $\chi_{c1}(3872)$ and $\psi(2S)$ production in pp collisions, Phys. Rev. Lett. **126**, 092001 (2021).

[51] J. M. Durham (LHCb Collaboration), Modification of $\chi_{c1}(3872)$ and $\psi(2S)$ production in pPb collisions at

$\sqrt{s_{NN}} = 8.16$ TeV, LHCb-CONF-2022-001, CERN-LHCb-CONF-2022-001 (2022).
[52] R. Rapp, D. Blaschke, and P. Crochet, Charmonium and bottomonium production in heavy-ion collisions, Prog. Part. Nucl. Phys. **65**, 209 (2010).
[53] R. Rapp, Bottomonium suppression in heavy-ion collisions and the in-medium strong force, Nucl. Sci. Tech. **34**, 63 (2023).
[54] F. Karsch, D. Kharzeev, and H. Satz, Sequential charmonium dissociation, Phys. Lett. B **637**, 75 (2006).
[55] S. Chatrchyan *et al.* (CMS Collaboration), Observation of sequential upsilon suppression in PbPb collisions [Phys. Rev. Lett. **109**, 222301 (2012)], Phys. Rev. Lett. **120**, 199903 (2018)].
[56] B. Aboona *et al.* (STAR Collaboration), Observation of sequential Υ suppression in Au+Au collisions at $\sqrt{s_{\rm NN}} = 200$ GeV with the STAR experiment, Phys. Rev. Lett. **130**, 112301 (2023).
[57] X. Du and R. Rapp, Sequential regeneration of charmonia in heavy-ion collisions, Nucl. Phys. A **943**, 147 (2015).
[58] L. Grandchamp and R. Rapp, Charmonium suppression and regeneration from SPS to RHIC, Nucl. Phys. A **709**, 415 (2002).
[59] A. Capella, L. Bravina, E. G. Ferreiro, A. B. Kaidalov, K. Tywoniuk, and E. Zabrodin, Charmonium dissociation and recombination at RHIC and LHC, Eur. Phys. J. C **58**, 437 (2008).
[60] X. Du, M. He, and R. Rapp, Color screening and regeneration of bottomonia in high-energy heavy-ion collisions, Phys. Rev. C **96**, 054901 (2017).
[61] K. Zhou, N. Xu, Z. Xu, and P. Zhuang, Medium effects on charmonium production at ultrarelativistic energies available at the CERN large hadron collider, Phys. Rev. C **89**, 054911 (2014).
[62] N. Armesto, B. Cole, C. Gale, W. A. Horowitz, P. Jacobs, S. Jeon, M. van Leeuwen, A. Majumder, B. Müller, G-Y. Qin, C. A. Salgado, B. Schenke, M. Verweij, X.-N. Wang, and U. A. Wiedemann, Comparison of jet quenching formalisms for a quark-gluon plasma 'brick', Phys. Rev. C **86**, 064904 (2012).
[63] C. Shen, Z. Qiu, H. Song, J. Bernhard, S. Bass, and U. Heinz, The iEBE-VISHNU code package for relativistic heavy-ion collisions, Comput. Phys. Commun. **199**, 61 (2016).
[64] C. Plumberg, The multiplicity dependence of pion interferometry in hydrodynamics, arXiv:2010.11957.
[65] S. F. Taghavi, Smallest QCD droplet and multiparticle correlations in p-p collisions, Phys. Rev. C **104**, 054906 (2021).
[66] W. Zhao, Y. Zhou, K. Murase, and H. Song, Searching for small droplets of hydrodynamic fluid in proton–proton collisions at the LHC, Eur. Phys. J. C **80**, 846 (2020).
[67] G. Aad *et al.* (ATLAS collaboration), Charged-hadron production in pp, p+Pb, Pb+Pb, and Xe+Xe collisions at $\sqrt{s_{\rm NN}} = 5$ TeV with the ATLAS detector at the LHC, J. High Energy Phys. 07 (2023) 074.
[68] C. Shen, J. F. Paquet, G. S. Denicol, S. Jeon, and C. Gale, Thermal photon radiation in high multiplicity p+Pb collisions at the large hadron collider, Phys. Rev. Lett. **116**, 072301 (2016).
[69] R. A. Lacey and N. Magdy, Scaling properties of the $\Delta\gamma$ correlator and their implication for detection of the chiral magnetic effect in heavy-ion collisions, arXiv:2206.05773.
[70] D. Oliinychenko and C. Shen, Resonance production in PbPb collisions at 5.02 TeV via hydrodynamics and hadronic afterburner, arXiv:2105.07539.
[71] S. Wang, W. Dai, B.-W. Zhang, and E. Wang, Z^0 boson associated b-jet production in high-energy nuclear collisions, Chin. Phys. C **47**, 054102 (2023).
[72] O. Garcia Montero, N. Löher, A. Mazeliauskas, K. Reygers, and J. Berges, Untangling the evolution of heavy ion collisions using direct photon interferometry, PoS **(HardProbes2020)**, 033 (2021).
[73] W. Dai, S. Wang, S.-L. Zhang, B.-W. Zhang, and E. Wang, Transverse momentum balance and angular distribution of $b\bar{b}$ dijets in Pb+Pb collisions, Chin. Phys. C **44**, 104105 (2020).
[74] I. M. Mitrankov, Y. A. Berdnikov, A. Y. Berdnikov, D. O. Kotov, M. M. Mitrankova, and N. Novitzky (PHENIX Collaboration), The ϕ meson production from small to large systems of ion collisions at $\sqrt{S_{NN}} = 200$ and 193 GeV, Phys. Scr. **97**, 054012 (2022).
[75] N. Abbasi, D. Allahbakhshi, A. Davody, and S. F. Taghavi, Standardized cumulants of flow harmonic fluctuations, Phys. Rev. C **98**, 024906 (2018).
[76] W. Zhao, L. Zhu, H. Zheng, C. M. Ko, and H. Song, Spectra and flow of light nuclei in relativistic heavy ion collisions at energies available at the BNL relativistic heavy ion collider and at the CERN large hadron collider, Phys. Rev. C **98**, 054905 (2018).
[77] X. Zhu, Spectra and elliptic flow of (multi-)strange hadrons at RHIC and LHC within viscous hydrodynamics+hadron cascade hybrid model Adv. High Energy Phys. **2016**, 4236492 (2016).
[78] R. A. Lacey, N. Magdy, P. Parfenov, and A. Taranenko, Scaling properties of background- and chiral-magnetically-driven charge separation in heavy ion collisions at $\sqrt{s_{\rm NN}} = 200$ GeV, arXiv:2203.10029.
[79] H.-J. Xu, W. Zhao, H. Li, Y. Zhou, L.-W. Chen, and F. Wang, Probing nuclear structure with mean transverse momentum in relativistic isobar collisions, Phys. Rev. C **108**, L011902 (2023).
[80] U. W. Heinz and J. Liu, Pre-equilibrium dynamics and heavy-ion observables, Nucl. Phys. A **956**, 549 (2016).
[81] P. Ru, G. Bary, and W.-N. Zhang, Pion transverse-momentum spectrum and elliptic anisotropy of partially coherent source, Phys. Lett. B **777**, 79 (2018).
[82] N.-b. Chang, ShanShan Cao, B.-y. Chen, S.-y. Chen, Z.-y. Chen, H.-T. Ding, M. He, Z.-q. Liu, L.-g. Pang, G.-y. Qin *et al.*, Physics perspectives of heavy-ion collisions at very high energy, Sci. China Phys. Mech. Astron. **59**, 621001 (2016).
[83] J. Li, H.-J. Xu, and H. Song, Noncritical fluctuations of (net) charges and (net) protons from the iEBE-VISHNU hybrid model, Phys. Rev. C **97**, 014902 (2018).
[84] H. Mehrabpour and S. F. Taghavi, Non-Bessel–Gaussianity and flow harmonic fine-splitting, Eur. Phys. J. C **79**, 88 (2019).
[85] Y. Li, S. Wang, and B.-W. Zhang, Longitudinal momentum fraction of heavy-flavor mesons in jets in high-energy nuclear collisions, Phys. Rev. C **108**, 024905 (2023).
[86] X. Zhu, F. Meng, H. Song, and Y.-X. Liu, Hybrid model approach for strange and multistrange hadrons in 2.76A TeV Pb+Pb collisions, Phys. Rev. C **91**, 034904 (2015).

[87] C. Mordasini, A. Bilandzic, D. Karakoç, and S. F. Taghavi, Higher order symmetric cumulants, Phys. Rev. C **102**, 024907 (2020).

[88] I. M. Mitrankov, E. V. Bannikov, A. Y. Berdnikov, Y. A. Berdnikov, and D. O. Kotov, Elliptic flow for φ-mesons in Cu+Au and U+U collisions, J. Phys.: Conf. Ser. **2103**, 012133 (2021).

[89] X. Zhu, Y. Zhou, H. Xu, and H. Song, Correlations of flow harmonics in 2.76A TeV Pb–Pb collisions, Phys. Rev. C **95**, 044902 (2017).

[90] S. Aronson, E. Borras, B. Odegard, R. Sharma, and I. Vitev, Collisional and thermal dissociation of J/ψ and Υ states at the LHC, Phys. Lett. B **778**, 384 (2018).

[91] H. Song, Y. Zhou, and K. Gajdosova, Collective flow and hydrodynamics in large and small systems at the LHC, Nucl. Sci. Tech. **28**, 99 (2017).

[92] J. Fu, Centrality dependence of mapping the hydrodynamic response to the initial geometry in heavy-ion collisions, Phys. Rev. C **92**, 024904 (2015).

[93] S. Acharya *et al.* (ALICE Collaboration), Neutral pion and η meson production in p-Pb collisions at $\sqrt{s_{\rm NN}} = 5.02$ TeV, Eur. Phys. J. C **78**, 624 (2018).

[94] D. Devetak, Dissipative phenomena in QCD plasma state created in heavy ion collisions, Eur. Phys. J. D **75**, 66 (2021).

[95] C. Shen, C. Park, J.-F. Paquet, G. S. Denicol, S. Jeon, and C. Gale, Direct photon production and jet energy-loss in small systems, Nucl. Phys. A **956**, 741 (2016).

[96] J. E. Bernhard, J. S. Moreland, S. A. Bass, J. Liu, and U. Heinz, Applying Bayesian parameter estimation to relativistic heavy-ion collisions: Simultaneous characterization of the initial state and quark-gluon plasma medium, Phys. Rev. C **94**, 024907 (2016).

[97] S. Acharya *et al.* (ALICE Collaboration), Production of charged pions, kaons, and (anti-)protons in Pb-Pb and inelastic *pp* collisions at $\sqrt{s_{NN}} = 5.02$ TeV, Phys. Rev. C **101**, 044907 (2020).

[98] S. Acharya *et al.* (ALICE Collaboration), Anisotropic flow of identified particles in Pb-Pb collisions at $\sqrt{s_{\rm NN}} = 5.02$ TeV, J. High Energy Phys. 09 (2018) 006.

[99] S. Acharya *et al.* (ALICE Collaboration), Centrality and pseudorapidity dependence of the charged-particle multiplicity density in Xe–Xe collisions at $\sqrt{s_{\rm NN}}$ =5.44TeV, Phys. Lett. B **790**, 35 (2019).

[100] L.-G. Pang, K. Zhou, N. Su, H. Petersen, H. Stöcker, and X.-N. Wang, An equation-of-state-meter of quantum chromodynamics transition from deep learning, Nat. Commun. **9**, 210 (2018).

[101] W. Zhao, H.-j. Xu, and H. Song, Collective flow in 2.76 A TeV and 5.02 A TeV Pb+Pb collisions, Eur. Phys. J. C **77**, 645 (2017).

[102] J. Adam *et al.* (ALICE Collaboration), Higher harmonic flow coefficients of identified hadrons in Pb-Pb collisions at $\sqrt{s_{\rm NN}} = 2.76$ TeV, J. High Energy Phys. 09 (2016) 164.

[103] J. Qian, U. W. Heinz, and J. Liu, Mode-coupling effects in anisotropic flow in heavy-ion collisions, Phys. Rev. C **93**, 064901 (2016).

[104] W. Zhao, Y. Zhou, H. Xu, W. Deng, and H. Song, Hydrodynamic collectivity in proton–proton collisions at 13 TeV, Phys. Lett. B **780**, 495 (2018).

[105] H.-J. Xu, Z. Li, and H. Song, High-order flow harmonics of identified hadrons in 2.76A TeV Pb + Pb collisions, Phys. Rev. C **93**, 064905 (2016).

[106] Y.-L. Du, K. Zhou, J. Steinheimer, L.-G. Pang, A. Motornenko, H.-S. Zong, X.-N. Wang, and H. Stöcker, Identifying the nature of the QCD transition in relativistic collision of heavy nuclei with deep learning, Eur. Phys. J. C **80**, 516 (2020).

[107] C. Shen, Z. Qiu, and U. Heinz, Shape and flow fluctuations in ultracentral Pb + Pb collisions at the energies available at the CERN large hadron collider, Phys. Rev. C **92**, 014901 (2015).